



## **Inhibitive effect of N,N'-bis(Salicylidene)-1,2-Diaminoethane and N,N'-bis(3-Methoxy Salicylidene)-1,2-Diaminoethane on the corrosion of AA6061 alloy in Hydrochloric acid**

**Sanaulla Pathapalya Fakrudeen\*<sup>1</sup> and Bheema Raju V<sup>2</sup>**

1. Department of Chemistry, HKBK College of Engineering, Nagawara, Bangalore -560045, Karnataka, **INDIA**

2. Department of Chemistry, Dr. Ambedkar Institute of Technology, Mallatha halli, Bangalore – 560056, **INDIA**

Email: [sanahkbk@gmail.com](mailto:sanahkbk@gmail.com)

Received on 24<sup>th</sup> June and finalized on 3<sup>rd</sup> July 2013.

### **ABSTRACT**

*The inhibitive effect of Schiff base compounds namely N, N'-bis (Salicylidene)-1, 2-Diaminoethane (Salen) and N, N'-bis (3-Methoxy Salicylidene)-1, 2 Diaminoethane (Msalen) on the corrosion of aluminium alloy AA6061 in presence of 1M Hydrochloric Acid was investigated using by Potentiodynamic polarization(PDP), electrochemical impedance spectroscopy(EIS) and weight loss method. The Potentiodynamic polarization study indicated that the two Schiff bases acted as mixed type inhibitors. The change in EIS parameters is indicative of adsorption of Schiff bases on aluminum alloy surface leading to the formation of protective layer. The weight loss study showed that the inhibition efficiency of these compounds increases with increase in concentration and vary with solution temperature and immersion time. The thermodynamic parameters were calculated to investigate the mechanism of corrosion inhibition. The effect of methoxy group on corrosion efficiency was observed from the results obtained between Salen and Msalen. The effectiveness of these inhibitors were in the order of Msalen>Salen. The adsorption of Schiff bases on AA6061 alloy surface in acid obeyed Langmuir adsorption isotherm. The surface characteristics of inhibited and uninhibited alloy samples were investigated by scanning electron microscopy (SEM) and atomic force microscopy (AFM).*

**Keywords:** Aluminum alloy, Corrosion inhibitors, Schiff base, Electrochemical techniques, Adsorption isotherms.

### **INTRODUCTION**

Aluminum and its alloys represent an important category of materials due to their high technological value and wide range of industrial applications, especially in aerospace, automobile and household industries. Aluminum alloys enjoy a wide range of commercial usage due to their numerous desirable properties such as excellent mechanical properties, high strength, low density, lightweight, high thermal conductivity. However, they are reactive materials and are prone to corrosion [1]. Owing to its wide applicability in industrial and every life, the electrochemical properties of aluminum and its alloys are the subject of many studies.

The most important problem in this area of research is related to the protection of aluminum and its alloys against corrosion. One of the most important methods against the corrosion is to use inhibitors. The effect

of inhibitor is to prevent the metal from the corrosive medium or to modify the electrode reactions that cause dissolution of the metal. Most of the efficient acid inhibitors are organic compounds that contain mainly nitrogen, sulphur or oxygen atoms in their structure. The inhibition efficiency of organic compounds is strongly dependent on the structure and chemical properties of the layer formed on conditions. Heterocyclic compounds are well known for their efficiencies as corrosion inhibitors and those containing nitrogen have been frequently referred to in the literature [2-5].

Some workers have studied corrosion inhibition efficiency of Schiff's bases for aluminium in HCl solution [6-9]. Among the compounds to have received attention as corrosion inhibitors for aluminium are Schiff bases derived from aliphatic and aromatic monoamines and diamines [10].

The aim of this study is to investigate the inhibition effect of some Schiff base compounds on the corrosion of AA60061 alloy in 1M HCl using weight loss, potentiodynamic polarization and electrochemical impedance spectroscopy techniques. The mode of adsorption and the corrosion inhibition mechanism are also discussed.

## MATERIALS AND METHODS

**Electrodes:** The alloy samples were procured from M/S. Fenfe Metallurgical, Bangalore, India. The typical chemical composition of AA6061 alloy in weight percentage is magnesium (0.8 -1.2), silicon (0.4 - 0.8), copper (0.15 -0.40), iron (0.7 Max), manganese (0.15 Max), titanium (0.15 Max) chromium (0.04- 0.35), zinc (0.25 Max), others (0.15 Max) and aluminum (Reminder) [11].

The alloy samples were cut into cylindrical test specimens and moulded in cold setting Acrylic resin exposing a surface area of 1.0 cm<sup>2</sup> for electrochemical measurements. For weight loss experiments the cylindrical alloy rods were cut into 2.4cm dia x 0.2cm height -circular cylindrical disc specimens using an abrasive cutting wheel and a 0.2cm mounting hole at the centre of the specimen was drilled. Before each experiment, the electrodes were abraded with a sequence of emery papers of different grades (600, 800, and 1200), washed with double distilled water, degreased with acetone and dried at 353±1 K for 30 min in a thermostated electric oven and stored in a moisture-free desiccator prior to use. The corrosive medium selected for this study was 1M hydrochloric acid, which was prepared from analytical grade 37 percent acid concentrated (Merck ) in double distilled water.

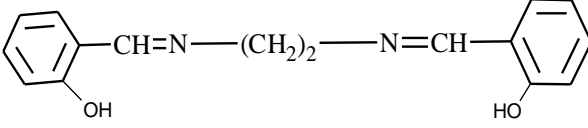
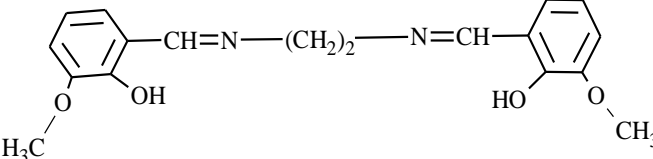
**Inhibitor:** The Schiff Bases were prepared by the condensation of respective aromatic aldehydes with each of diamines as per the reported procedure [12-13]. All reagents used were of analytical grade procured from Sigma Aldrich. N,N'-bis(Salicylidene)-1,2-Diaminoethane (Salen) was prepared by slow addition of Salicylaldehyde (2 mmol) in 30 mL methanol over a solution of 1,2-diaminoethane (1mmol) in 30 mL methanol and N,N'-bis(3-MethoxySalicylidene)-1,2-Diaminoethane (Msalen) by slow addition of Methoxysalicylaldehyde (2 mmol) in 30 mL methanol over a solution of 1,2-diaminoethane (1 mmol) in 30 mL methanol taken in a 250 mL condensation flask. In each case, 2-3 drops of acetic acid were added to the mixture of aldehyde and diamine with stirring at constant temperature of 298±1 K for 1 hour. Further the mixture was refluxed for 4-5 hours on a water bath, heating occasionally to improve the yield of the product. The reaction mixture was cooled to room temperature overnight and the colored compound was filtered off and dried. The compounds were recrystallized with ethanol. The product identity was confirmed *via* melting points, Fourier transform infrared spectroscopy (FT-IR) and Proton Nuclear Magnetic Resonance (<sup>1</sup>H NMR). The structure, molecular formula, molecular mass and melting points are shown in table-1.

### N,N'-bis(Salicylidene)-1,2-Diaminoethane

IR (KBr cm<sup>-1</sup>): 3415(OH), 3040(=C-H), 2860(-CH), 1628(C=N).

<sup>1</sup>HNMR (CDCl<sub>3</sub>): δ 3.94 (s, 4H, -CH<sub>2</sub>-N), 6.83-7.3 (m, 8H, ArH). 8.35(s, 2H, N=CH), 13.17 (s, 1H, OH),

**N,N'-bis(3-Methoxy Salicylidene)-1,2- Diaminoethane**IR (KBr  $\text{cm}^{-1}$ ): 3443(OH), 3004(=C-H), 2896(-CH), 1628(C=N), 1246(-OCH<sub>3</sub>)<sup>1</sup>HNMR (CDCl<sub>3</sub>):  $\delta$  3.88(s, 6H, -OCH<sub>3</sub>),  $\delta$  3.96 (s, 4H, -CH<sub>2</sub>-N), 6.75–6.91 (m, 6H, ArH). 8.33(s, 2H, N=CH), 13.56 (s, 1H, OH),**Table 1.** Schiff bases

Structure and Name	Molecular Formula	Molecular Mass	Melting Point
 N,N'-bis(Salicylidene)-1,2-Diaminoethane (Salen)	C <sub>16</sub> H <sub>16</sub> N <sub>2</sub> O <sub>2</sub>	268.31	129°C
 N,N'-bis(3-Methoxy Salicylidene)-1,2-Diaminoethane (Msalen)	C <sub>18</sub> H <sub>20</sub> N <sub>2</sub> O <sub>4</sub>	328.37	180°C

**Electrochemical measurements:** The working electrode with well defined area 1 cm<sup>2</sup> was abraded with a sequence of emery papers of different grades (600, 800, and 1200), degreased with acetone, washed with double distilled water and dried before immersing in the corrosion medium. The electrochemical measurements were performed in a conventional three electrode Pyrex glass cell consisting of aluminium alloy as working electrode (WE), platinum counter electrode (CE) and a saturated calomel electrode (SCE) as the reference electrode. The reference electrode was connected to a Luggin capillary to minimize IR drop. All the values of potential were referred to SCE. The electrochemical measurements were performed using CHI660c electrochemical workstation.

**Potentiodynamic Polarization (PDP) measurements:** Tafel plots were obtained by polarizing the electrode potential automatically from – 250 to + 250 mV with respect to open circuit potential (OCP) at a scan rate 1mV s<sup>-1</sup>. The linear Tafel segments of anodic and cathodic curves were extrapolated to corrosion potential (E<sub>corr</sub>) to obtain corrosion current densities (I<sub>corr</sub>). The inhibition efficiency was evaluated from the I<sub>corr</sub> values using the following relationship (1):

$$\mu_P \% = \frac{I_{corr}^0 - I_{corr}}{I_{corr}^0} \times 100 \quad \dots \dots \dots (1)$$

Where, I<sub>corr</sub><sup>0</sup> and I<sub>corr</sub> are values of corrosion current densities in absence and presence of inhibitor respectively.

**Electrochemical Impedance Spectroscopy (EIS) measurements:** EIS measurements were carried out in a frequency range from 100 kHz to 1.0 mHz with small amplitude of 10mV peak -to-peak, using AC signal at OCP. The impedance data was analyzed using Nyquist plot and Echem software ZSimpWin version 3.21 was used for data fitting to obtain the equivalent circuit model. The inhibition efficiency ( $\mu_{R_{ct}}$  %) was calculated from the charge transfer resistance (R<sub>ct</sub>) values using following equation (2):

$$\mu_{R_{ct}} \% = \frac{R_{ct}^i - R_{ct}^0}{R_{ct}^i} \times 100 \quad \dots \dots \dots (2)$$

Where, R<sub>ct</sub><sup>i</sup> and R<sub>ct</sub><sup>0</sup> are the charge transfer resistance in presence and absence of inhibitor, respectively.

**Weight loss measurement:** Weight loss measurements were performed on aluminium alloys AA6061 and AA6063 as per ASTM method [14]. Before each experiment, the electrodes were abraded with a sequence of emery papers of different grades (600, 800, and 1200), degreased with acetone, washed with double distilled water, and dried at 353 K for 30 min in a thermostat electric oven and stored in a moisture-free desiccator prior to use. The weight of the specimen was measured before exposing it to the corrodent solution on a Shimadzu AX 200 Electronic Analytical weighing balance. The volume of the test solution was kept large excess over per square centimeter of the test specimen to avoid any appreciable change in its corrosivity during the test, either through exhaustion of corrosive constituent or by accumulation of corrosion products that might affect further corrosion. The studies were carried out under varying conditions of immersion time, solution temperature, and concentrations of inhibitor and acid. After a definite immersion time, the specimen was taken out and washed with running water and immersed in 70% nitric acid for 3 minutes. The corrosion product on the alloy surface was removed mechanically by gently rubbing with nylon tooth brush. The specimen was then dried at 353 K and loss in weight was recorded by weighing up to 0.1mg accuracy. Constant temperature bath was used to study the weight loss at desired temperatures ( $\pm 1$ K). The test solution was taken in lidded glass bottle fixed with a condenser.

The test specimens were immersed in 100 mL 1M hydrochloric acid solution in absence and presence of different concentrations (25,50,75 and 100 ppm) of Schiff bases at different temperature ranges (303, 313, 323 and  $333\pm 1$  K). The difference in weight for exposed period of 2, 4, 6 and 8 hours was taken as the total weight loss. The weight loss experiments were carried out in triplicate and average values were recorded.

**Calculation of corrosion rate (CR):** The average corrosion rate was evaluated as per ASTM Method [14] equation (3) in mmpy.

$$CR = \frac{K \times W}{DAT} \dots\dots\dots(3)$$

Where, CR= Corrosion rate in mmpy, K = a constant ( $8.76 \times 10^4$ ), W = Weight loss in grams, D = Density in  $g/cm^3$ , A= Surface area of test specimen in  $cm^2$  and T = Time of exposure in hours.

**Calculation inhibition efficiency:** The percentage of inhibition efficiency ( $\mu_{WL\%}$ ) and the degree of surface coverage ( $\theta$ ) were calculated using equations (4) and (5) respectively :

$$\mu_{WL} \% = \frac{W_0 - W_i}{W_0} \times 100 \dots\dots\dots(4)$$

$$\theta = \frac{W_0 - W_i}{W_0} \dots\dots\dots(5)$$

Where,  $W_0$  and  $W_i$  are the weight loss values of aluminium alloy sample in the absence and presence of the inhibitor and  $\theta$  is the degree of surface coverage of the inhibitor.

**Scanning electron microscopy (SEM) studies:** The surface morphology of the corroded surface in the presence and absence of inhibitors were studied using scanning electron microscope (SEM) JSM-840A-JEOL. To understand the surface morphology of the aluminium alloy in the absence and presence of inhibitors, the following cases were examined. The specimens were thoroughly washed with double distilled water before mounting on the slide.

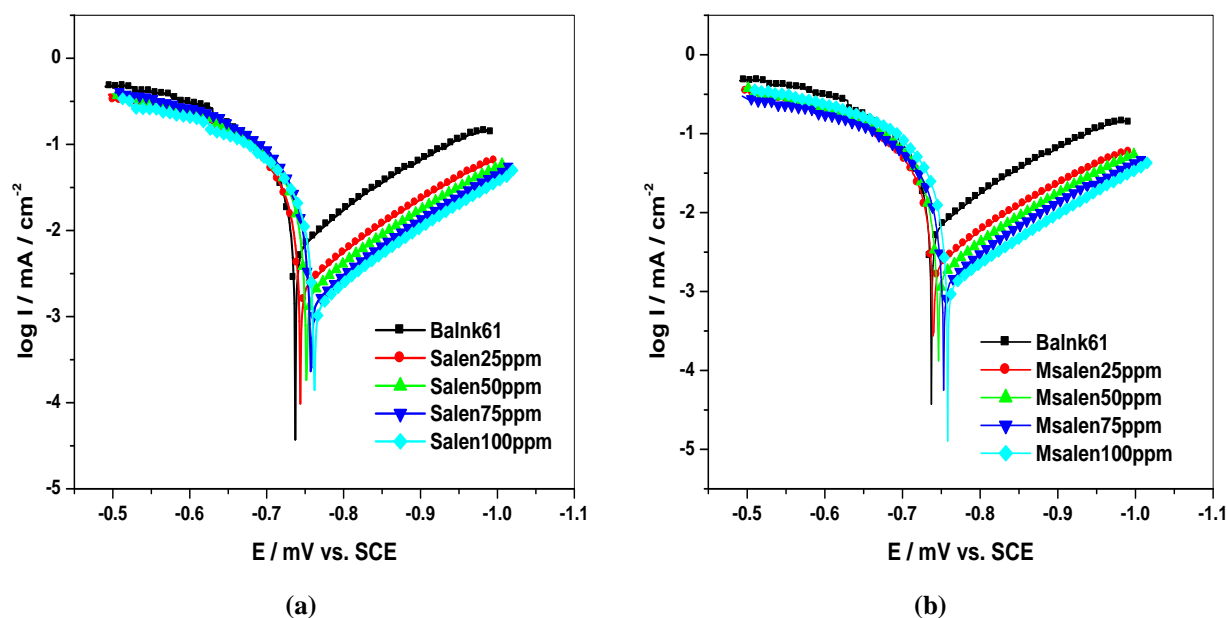
- (i) Polished aluminium alloy specimen.
- (ii) Aluminium alloy specimen dipped in 1M HCl.
- (iii) Aluminium alloy specimen dipped in 1M HCl containing 100 ppm of Schiff base.

**Atomic Force Microscopy (AFM) studies:** The surface topography of the alloy surface in the presence and absence of inhibitors were studied using Atomic Force Microscopy Nanosurf<sup>®</sup> AFM, NANOSURF AG, Switzerland. Semi contact mode was used with the tip of the modular scanning probe mounted on 100 $\mu$ m long, single beam cantilever with resonating frequency in the range 240-255 kHz and the corresponding spring constant 20  $Nm^{-1}$ . All the images contained of 256 x 256 data points in the area of

12.5 x 12.5  $\mu\text{m}^2$ . The measurements were performed, displayed, and evaluated using the Easy Scan 2 SPM Control Software Version 3.0.

## RESULTS AND DISCUSSION

**Potentiodynamic polarization (PDP) measurements:** The polarization behaviour of AA6061 alloy specimens in 1M hydrochloric acid, in the absence and in the presence of different concentrations (25 -100 ppm) of Salen and Msalen at  $303\pm 1$  K was carried out in order to study the anodic and cathodic reactions. The Fig.1 (a) and (b) represents potentiodynamic polarization curves (Tafel plots) of AA6061 alloy in 1M hydrochloric acid in absence and presence of various concentrations of Salen and Msalen at  $303\pm 1$  K respectively. The potentiodynamic polarization parameters like corrosion potential ( $E_{\text{corr}}$ ), corrosion current density ( $I_{\text{corr}}$ ), cathodic and anodic Tafel slopes ( $b_a$  and  $b_c$ ) were calculated from Tafel plots. The Potentiodynamic polarization parameters associated with the polarization measurements of Salen and Msalen are listed in Table 2. It is observed from the PDP results that, with increase in concentration of inhibitors, the curves are shifted to lower current density ( $I_{\text{corr}}$ ) regions and the corrosion potential ( $E_{\text{corr}}$ ) values do not show any appreciable shift i.e. not more than 85 mV with respect to corrosion potential of the blank solution, which suggest that both inhibitors acted as mixed type [15, 16]. But the cathodic curves are more polarized indicating the retardation of cathodic reduction rate and hence, Schiff bases influenced cathodic reactions more rather than anodic reaction and predominantly act as cathodic inhibitors [17, 18]. This can probably be due to the adsorption of protonated Schiff base molecules on the cathodic and anodic sites. The inhibition efficiency Msalen is greater than Salen.

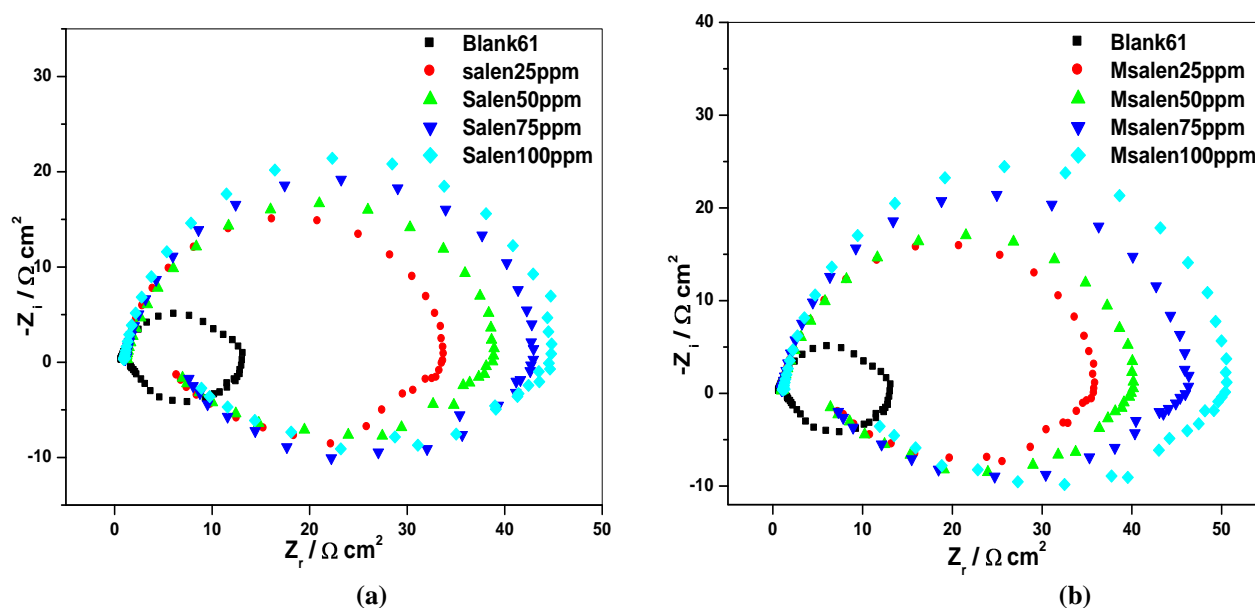


**Figure 1.** Potentiodynamic polarization curves (Tafel plots) of AA6061 alloy in 1M hydrochloric acid in absence and presence of various concentrations of (a) Salen and (b) Msalen at  $303\pm 1$  K.

**Table 2.** Potentiodynamic polarization parameters of AA6061 alloy in 1M hydrochloric acid in absence and presence of various concentrations of (a) Salen and (b) Msalen at 303±1K.

Tafel data						
Inhibitor	Concentration (ppm)	$-E_{\text{corr}}$ (mV vs. SCE)	$I_{\text{corr}}$ ( $\text{mA cm}^{-2}$ )	$b_c$ ( $\text{mV dec}^{-1}$ )	$b_a$ ( $\text{mV dec}^{-1}$ )	$\mu_p\%$
Salen	0	737	9.27	189	68	---
	25	744	3.54	191	76	61.8
	50	752	3.22	194	79	65.2
	75	758	2.81	197	81	69.6
	100	762	2.53	198	86	72.7
Msalen	25	740	3.29	194	81	64.5
	50	746	2.99	196	88	67.7
	75	753	2.56	199	91	72.4
	100	758	2.25	204	95	75.7

**Electrochemical impedance spectroscopy:** The effect of the inhibitor concentration on the impedance behavior of AA6061 alloy in 1M hydrochloric acid was studied and Nyquist plots of AA6061 in absence and presence of various concentrations of Salen and Msalen are given in Fig. 2 (a) and (b). It is clear from the Fig.2 that the impedance diagrams obtained yield a semicircle shape. This indicates that the corrosion process is mainly controlled by charge transfer. The general shape of the Nyquist plots is similar, with a large capacitive loop at higher frequencies and inductive loop at lower frequencies. The similar impedance plots have been reported for the corrosion of aluminium and its alloys in hydrochloric acid [19-25]. The Nyquist plot with a depressed semicircle with the center under the real axis is characteristic property of the solid electrode and this kind of phenomenon is known as the dispersing effect [26-27].

**Figure 2** Nyquist plot for AA6061 alloy in 1M hydrochloric acid in absence and presence of various concentrations of (a) Salen and (b) Msalen at 303±1 K.

An equivalent circuit fitting of five elements used to simulate the measured impedance data of AA6061 alloy is depicted in Fig.3. The equivalent circuit includes solution resistance  $R_s$ , charge transfer resistance  $R_{ct}$ , inductive elements  $R_L$  and  $L$ . The circuit also consists of constant phase element, CPE ( $Q$ ) in parallel to the parallel resistors  $R_{ct}$  and  $R_L$ , and  $R_L$  is in series with the inductor  $L$ .

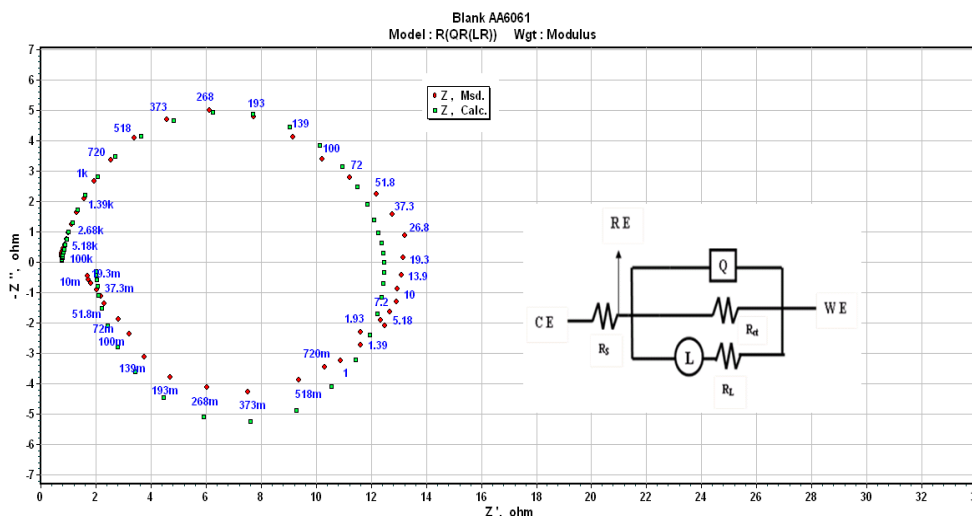


**Figure 3** The equivalent circuit model used to fit the experimental impedance data.

The impedance spectra for the aluminium alloy in absence and presence of the inhibitor are depressed. The deviation of this kind is referred as frequency dispersion, and has been attributed to inhomogeneous of solid surface of aluminium alloy. Assumption of a simple  $R_{ct} - C_{dl}$  is usually a poor approximation especially for systems showing depressed semicircle behavior due to non-ideal capacitive behaviour of solid electrodes [28]. The capacitor in the equivalent circuit can be replaced by a constant phase element (CPE), which is a frequency dependent element and related to surface roughness. CPE is substituted for the respective capacitor of  $C_{dl}$  in order to give a more accurate fit. The impedance function of a CPE is defined in impedance [29] representation as (6).

$$Z_{CPE} = \frac{1}{(Y_0 j \omega)^n} \dots\dots\dots (6)$$

Where,  $Y_0$  is magnitude of CPE,  $n$  is exponent of CPE and are frequency independent, and  $\omega$  is the angular frequency for which  $-Z''$  reaches its maximum value,  $n$  is dependent on the surface morphology :

$-1 \leq n \leq 1$ .  $Y_0$  and  $n$  can be calculated by the equation proved by Mansfeld et al [30].

The double layer capacitance ( $C_{dl}$ ) can be calculated [31] from the equation (7).

$$C_{dl} = Y_0 (\omega_{max})^{n-1} \dots\dots\dots (7)$$

Where  $C_{dl}$  is the double layer capacitance and  $\omega_{max}$  is the angular frequency at which  $-Z''$  reaches maximum and  $n$  is the CPE exponent.

The electrochemical impedance parameters  $R_s$ ,  $R_{ct}$ ,  $R_L$ ,  $L$ ,  $\omega$ , CPE,  $n$  and  $C_{dl}$  are listed in Table 3. The inhibition efficiency was evaluated by  $R_{ct}$  and  $C_{dl}$  values of the impedance data, it is shown from Table 3 that charge transfer resistance ( $R_{ct}$ ) of inhibited system increased and double layer capacitance ( $C_{dl}$ ) decreased with increase in inhibitor concentration. This was due to adsorption of Schiff base molecule on the alloy surface, the adsorbed inhibitor blocks either cathodic or anodic reaction or both by formation of physical barrier, which reduces alloy reactivity. The effect of inhibitor may be due to changes in electric double layer at the interface of solution and alloy electrode. The decrease in double layer capacitance ( $C_{dl}$ ) can be caused by decrease in local dielectric constant and /or increase in the thickness of electrical double layer, this suggest that the Schiff base molecules inhibit the aluminium alloy by adsorption at the alloy-acid interface. It is evident that the inhibition efficiency increases with increase in inhibitor concentration which is in good agreement with the potentiodynamic polarization results. The charge transfer resistance ( $R_{ct}$ ) and double layer capacitance ( $C_{dl}$ ) values indicate that the Msalen inhibit AA6061 alloy more efficiently than Salen.

**Table 3.** Electrochemical impedance parameters of AA6061 alloy in 1M hydrochloric acid in absence and presence of various concentrations of (a) Salen and (b) Msalen at 303±1 K

EIS data										
Inhibitor	Concentration (ppm)	$R_s$ ( $\Omega \text{ cm}^{-2}$ )	$R_{ct}$ ( $\Omega \text{ cm}^{-2}$ )	$R_L$ ( $\Omega \text{ cm}^{-2}$ )	L ( $\text{H cm}^{-2}$ )	$\omega$ (Hz)	CPE ( $\mu\text{F cm}^{-2}$ )	$n$	Cdl ( $\mu\text{F cm}^{-2}$ )	$\mu_{Ret}$ %
Salen	0	1.10	12	1.37	5.98	4.9	123	0.8905	84.5	---
	25	1.09	32	8.9	49	14	111	0.8939	69.0	62.5
	50	1.11	36	10.7	63	16	91	0.9115	60.5	66.6
	75	1.13	41	11.5	79	19	77	0.9179	52.0	70.7
	100	1.18	43	15.1	108	22	63	0.9285	44.2	72.1
Msalen	25	1.17	35	11.5	65	16	73	0.9008	46.3	65.7
	50	1.19	38	12.7	69	17	70	0.9032	44.5	68.4
	75	1.23	45	14.3	87	21	65	0.9063	41.1	73.3
	100	1.27	51	20.9	134	24	58	0.9114	37.2	76.5

**Weight loss measurements:** The corrosion inhibition of AA6061 alloy in 1M hydrochloric acid in absence and presence of Salen and Msalen was studied by monitoring its weight loss as a function of various concentrations of inhibitor, immersion time and solution temperature. The weight loss experimental parameters weight loss ( $\Delta w$ ), percentage of inhibition efficiency ( $\mu_{WL}\%$ ), Corrosion Rate (C.R.) in mmpy and degree of surface coverage ( $\theta$ ) for AA6061 in 1M hydrochloric acid in absence and presence of various concentration of (a) Salen and (b) Msalen Schiff bases at 2 hours of exposure time and at different temperature are shown in Table. 4.

**Effect of inhibitor concentration:** The variation of inhibition efficiency ( $\mu_{WL}\%$ ) with inhibitor concentration is shown in Fig.4 (a). Increase in inhibition efficiency at higher concentration of inhibitor may be attributed to larger coverage of alloy surface with inhibitor molecules. The maximum inhibition efficiency was achieved at 100 ppm and a further increase in inhibitor concentration caused no appreciable change in performance.

**Effect of immersion time:** The effect of immersion time on the inhibition efficiency is shown in Fig.4 (b). All the tested Schiff bases show a decrease in inhibition efficiency with increase in immersion time from 2 to 8 hours. This indicates desorption of the Schiff base over a longer test period and may be attributed to various other factors such as formation of less persistent film layer on the alloy surface, and increase in cathodic reaction or increase in ferrous ion concentration [32].

**Effect of temperature:** The influence of temperature on inhibition efficiency of two Schiff bases compounds is shown in Fig.4 (c). The inhibition efficiency for the two Schiff base compounds decreases with increase in temperature from 303 to 333±1 K. The decrease in inhibition efficiency with rise in temperature may be attributed to desorption of the inhibitor molecules from alloy surface at higher temperatures and higher dissolution rates of aluminium at elevated temperatures.

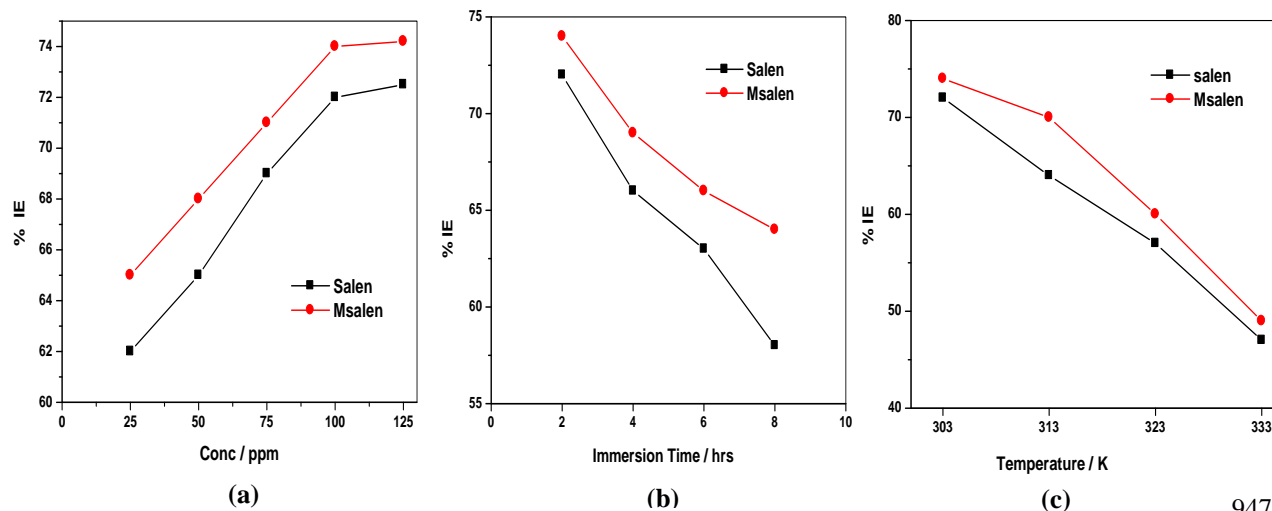




**Figure 4.** Variation of inhibition efficiency with (a) Inhibitor concentration (b) Exposure time (c) Temperature in 1M hydrochloric acid for Salen and Msalen.

**Thermodynamic activation parameters:** Thermodynamic activation parameters are important to study the inhibition mechanism. The activation energy ( $E_a$ ) is calculated from the logarithm of the corrosion rate in acidic solution is a linear function of  $(1/T)$  -Arrhenius equation (8):

$$\log (CR) = -E_a/2.303R \dots\dots\dots (8)$$

Where,  $E_a$  is the apparent effective activation energy, R is the universal gas constant and A is the Arrhenius pre exponential factor.

**Table 4.** Weight loss parameters for AA6061 in 1M hydrochloric acid in the absence and presence of various concentrations of Salen and Msalen at 2 hours of exposure time and at different temperatures.

Inhibitor	Temperature (K)	Concentration (ppm)	Weight loss (mg)	C.R. (mmpy)	$\mu_{WL}\%$	$\theta$
Salen	303	Blank	339.2	519.1	---	---
		25	128.9	197.3	62	0.62
		50	118.7	181.7	65	0.65
		75	105.2	160.9	69	0.69
		100	95.0	145.4	72	0.72
	313	Blank	575.5	880.7	---	---
		25	270.5	413.9	53	0.53
		50	253.2	387.5	56	0.56
		75	236.0	361.1	59	0.59
		100	207.2	317.1	64	0.64
	323	Blank	937.6	1434.9	---	---
		25	525.1	803.5	44	0.44
		50	487.6	746.1	48	0.48
		75	450.0	688.8	52	0.52
		100	403.2	617.0	57	0.57
	333	Blank	1412	2161.1	---	---
		25	903.7	1383.1	36	0.36
		50	847.3	1296.6	40	0.40
		75	776.7	1188.6	45	0.45
		100	748.4	1145.4	47	0.47
Msalen	303	25	118.7	181.7	65	0.65
		50	108.5	166.1	68	0.68
		75	98.4	150.5	71	0.71
		100	88.2	135.0	74	0.74
	313	25	247.5	378.7	57	0.57
		50	212.9	325.9	63	0.63
		75	195.7	299.5	66	0.66
		100	172.7	264.2	70	0.70
	323	25	487.6	746.1	48	0.48
		50	440.7	674.4	53	0.53
		75	412.5	631.4	56	0.56
		100	375.0	574.0	60	0.60
	333	25	875.5	1339.9	38	0.38
		50	819.0	1253.4	42	0.42
		75	762.5	1167.0	46	0.46
100		720.2	1102.1	49	0.49	

Plots of logarithm of corrosion rate obtained by weight loss measurement *versus*  $1/T$  gave straight lines and slope equal to  $(-E_a/2.303R)$  as shown in Fig. 5(a) and (b) for Salen and Msalen respectively. The  $E_a$  values calculated are listed in Table 5.

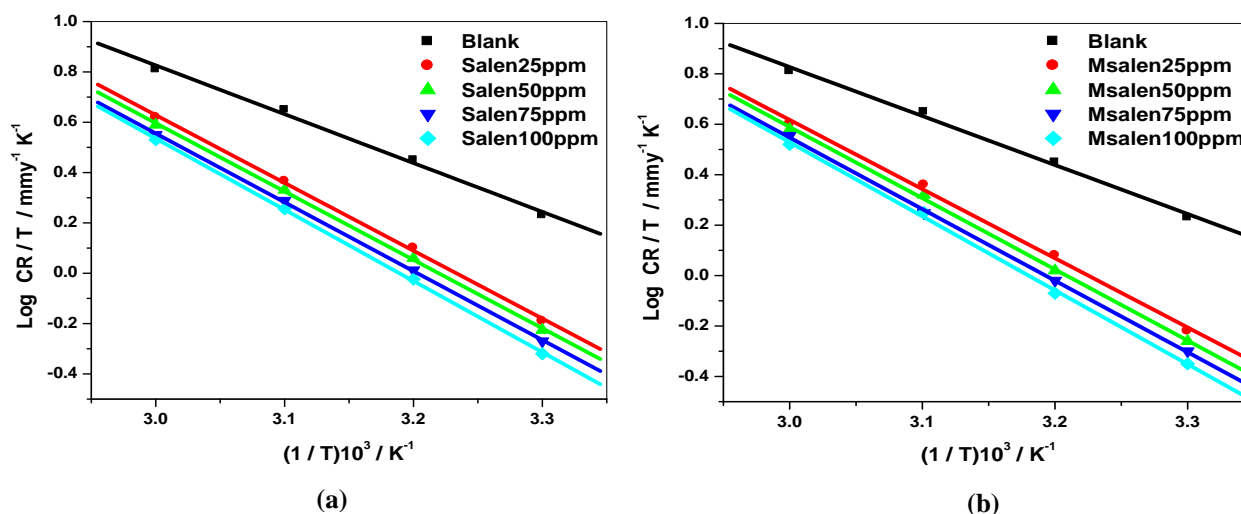


**Figure 5.** Arrhenius plot of log CR *versus*  $1/T$  in absence and presence of (a) Salen and (b) Msalen

A plot of  $\log (CR/T)$  *versus*  $1/T$  gave a straight line, Figs. 6(a) and (b) with a slope of  $(-\Delta H^*/2.303 R)$  and an intercept of  $[(\log (R/Nh) + (\Delta S^*/2.303 R))]$ , from which the values of  $\Delta S^*$  and  $\Delta H^*$  were calculated. The straight lines were obtained according to transition state equation (9):

$$CR = \frac{RT}{Nh} \exp\left(-\frac{\Delta H^*}{RT}\right) \exp\left(\frac{\Delta S^*}{R}\right) \dots\dots\dots (9)$$

Where,  $h$  is the Planck constant,  $N$  is the Avogadro number,  $\Delta S^*$  is entropy of activation and  $\Delta H^*$  is the enthalpy of activation. The  $\Delta S^*$  and  $\Delta H^*$  values calculated are listed in table-5.

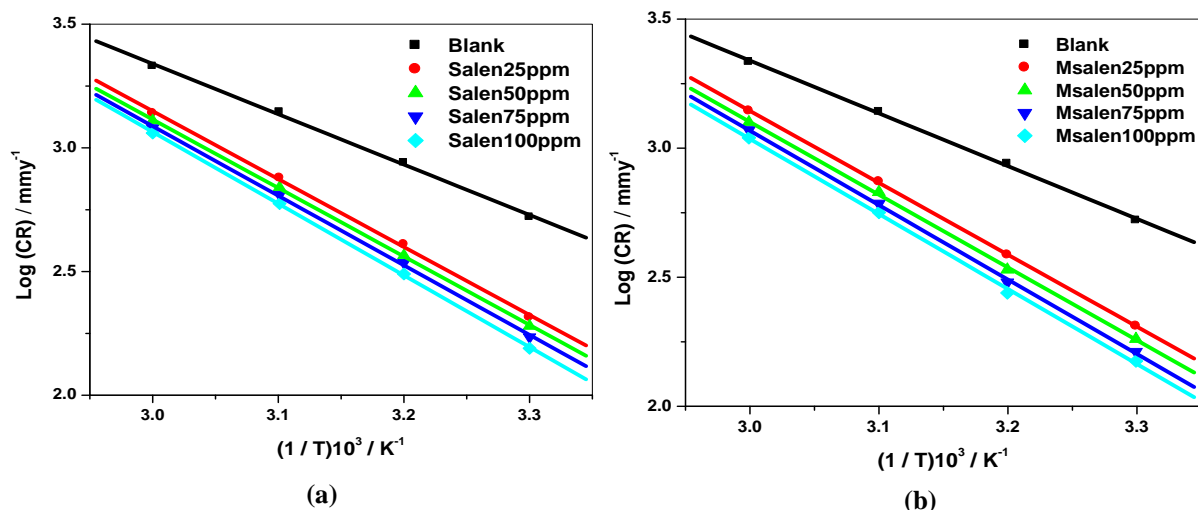


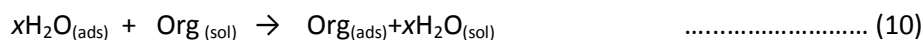
**Figure 6.** Arrhenius plot of  $\log (CR/T)$  *versus*  $1/T$  in absence and presence of (a) Salen and (b) Msalen

**Table 5.** Thermodynamic parameters of activation of AA6061 in 1M hydrochloric acid in presence and absence of different concentrations of Salen and Msalen.

Inhibitor	Concentration (ppm)	E <sub>a</sub> (kJmol <sup>-1</sup> )	ΔH* (kJmol <sup>-1</sup> )	ΔS* (J mol <sup>-1</sup> K <sup>-1</sup> )
Salen	Blank	39.00	37.06	-70.39
	25	52.59	51.50	-30.74
	50	53.01	52.04	-30.09
	75	53.86	52.40	-29.78
	100	55.50	54.21	-24.75
Msalen	25	53.34	52.52	-28.25
	50	53.98	54.06	-24.17
	75	55.21	54.32	-24.19
	100	56.61	56.16	-19.01

The E<sub>a</sub> values of aluminium alloy in 1M hydrochloric acid in the presence of Schiff base compounds are higher than those in the absence of Schiff bases indicating that the energy barrier for the corrosion reaction increases. It is also indicated that the whole process is controlled by surface reaction [33] since, the activation energies of the corrosion process are above 20 kJmol<sup>-1</sup>. The adsorption of the inhibitor on the electrode surface leads to the formation of a physical barrier between the alloy surface and the corrosion medium, blocking the charge transfer, and thereby reducing the alloy reactivity in the electrochemical reactions of corrosion. The increase in the E<sub>a</sub> values, with increasing inhibitor concentration is attributed to physical adsorption of inhibitor molecules on the alloy surface [34]. In other words, the adsorption of inhibitor on the electrode surface leads to formation of a physical barrier that reduces the alloy dissolution in electrochemical reactions [35]. The decrease in the inhibition efficiency of Schiff bases with the increase in temperature can be considered to be because of the decrease in the extent of adsorption of the inhibitor on the alloy surface with the increase in temperature, and corresponding increase in corrosion rate as a greater area of the alloy surface is exposed to the corrosion medium. The observations also support the view that the inhibitor is adsorbed on the alloy surface through physisorption [36, 37]. The values of enthalpy of activation (ΔH\*) are positive; this indicates that the corrosion process is endothermic. The values of entropy of activation (ΔS\*) are higher in the presence of inhibitor than those in the absence of inhibitor. The increase in values of ΔS\* reveals that an increase in randomness occurred on going from reactants to the activated complex [38-40]. This might be result of the adsorption of organic inhibitor molecules from the acidic solution which could be regarded as a quasi-substitution process between the organic molecule in the aqueous phase and water molecules at electrode surface.

**Adsorption isotherms:** It is generally assumed that the adsorption of the inhibitor at the interface of alloy and solution is the first step in the mechanism of inhibition aggressive media. It is also widely acknowledged that adsorption isotherms provide useful insights into the mechanism of corrosion inhibition. The investigated compounds inhibit the corrosion by adsorption at the alloy surface. Theoretically, the adsorption process has been regarded as a simple substitution adsorption process, in which an organic molecule in the aqueous phase substitutes the water molecules adsorbed on the alloy surface [41].



Where Org<sub>(sol)</sub> and Org<sub>(ads)</sub> are the organic molecules in the solution and adsorbed on the alloy surface, respectively; H<sub>2</sub>O<sub>(ads)</sub> and H<sub>2</sub>O<sub>(sol)</sub> are the water molecules on alloy surface and in the solution, respectively; and x is the number of water molecules replaced by the organic molecules. It is essential to know the mode of adsorption and adsorption isotherm that can give important information on the interaction of inhibitor and alloy surface.

The surface coverage (θ) values calculated from weight loss data for different concentrations of Schiff bases was used to explain the best adsorption isotherm. The value of surface coverage (θ) was tested graphically for fitting a suitable adsorption isotherm. Attempts were made to fit surface coverage (θ)

values of various isotherms including Langmuir, Freundlich and Temkin isotherms. Among three adsorption isotherms obtained, the best fitted isotherm was the Langmuir adsorption isotherm ( $C_{(inh)}/\theta$  vs.  $C_{(inh)}$ ) as shown in Fig.7(a) with the linear regression coefficient values ( $R^2$ ) in the range of 0.9990 - 0.9992. The Langmuir adsorption isotherm can be expressed by following equation (11).

$$\frac{C_{inh}}{\theta} = \frac{1}{K_{(ads)}} + C_{inh} \quad \dots\dots\dots (11)$$

Where  $C_{(inh)}$  is inhibitor concentration and  $K_{(ads)}$  is an equilibrium constant for adsorption and desorption. The  $K_{(ads)}$  was calculated from the intercepts of the straight lines on the  $C_{(inh)}/\theta$  axis and standard free energy of adsorption of inhibitor  $\Delta G_{ads}^0$  was calculated using the relation (12).

$$\Delta G_{ads}^0 = -RT \ln(55.5 K_{ads}) \quad \dots\dots\dots (12)$$

To calculate heat of adsorption ( $\Delta H_{ads}^0$ ) and entropy of adsorption ( $\Delta S_{ads}^0$ ),  $\ln K_{(ads)}$  versus  $1/T$  was plotted as shown in Fig.7(b). The straight lines were obtained with a slope equal to  $(-\Delta H_{ads}^0 / R)$  and intercept equal to  $(\Delta S_{ads}^0 / R + \ln 1/55.5)$ . The values of equilibrium constant ( $K_{(ads)}$ ), standard free energy of adsorption ( $\Delta G_{ads}^0$ ), enthalpy of adsorption ( $\Delta H_{ads}^0$ ) and entropy of adsorption ( $\Delta S_{ads}^0$ ) are listed in table 6.

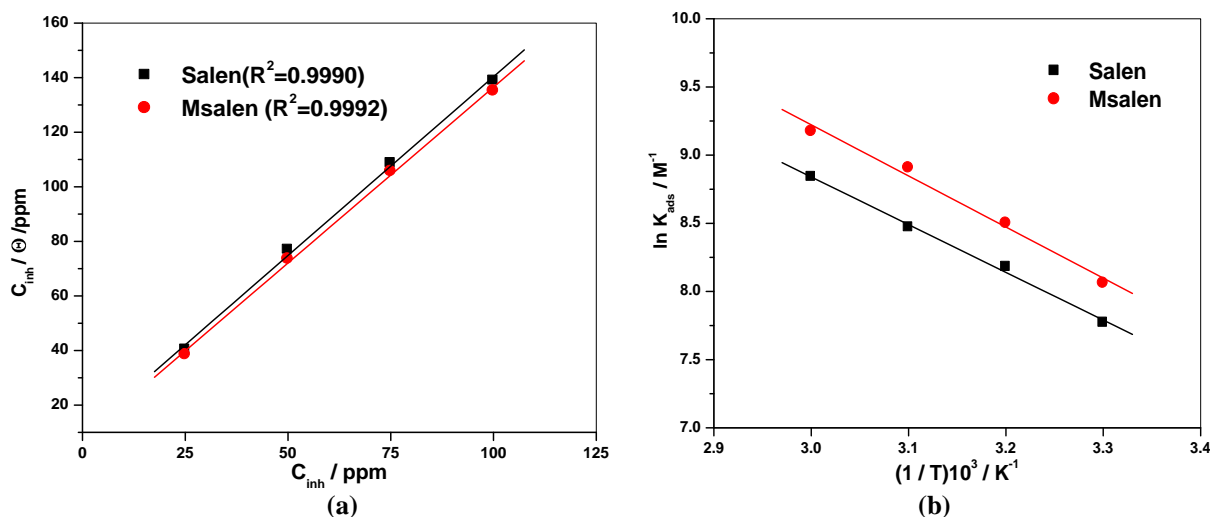


Figure 7 (a) Langmuir adsorption isotherm plot and (b) Heat of adsorption isotherm plot for Salen and Msalen.

Table 6. Thermodynamic parameters for the adsorption of inhibitor in 1M hydrochloric acid AA6061 alloy surface at different temperature.

Inhibitor	Concentration (ppm)	Temperature (K)	$K_{ads}$ ( $10^3 M^{-1}$ )	$\Delta G_{ads}^0$ ( $kJmol^{-1}$ )	$\Delta H_{ads}^0$ ( $kJmol^{-1}$ )	$\Delta S_{ads}^0$ ( $Jmol^{-1}$ )
Salen	100	303	6.89	-32	29.1	194
		313	4.77	-32		
		323	3.55	-33		
		333	2.38	-33		
Msalen	100	303	9.33	-33	31.2	204
		313	7.65	-33		
		323	4.92	-34		
		333	3.15	-34		

The negative values of standard free of adsorption indicated spontaneous adsorption of Schiff bases on aluminium alloy surface and stability of the adsorbed layer on the alloy surface. Generally the values of  $\Delta G_{ads}^0$  less than  $-20 kJmol^{-1}$  are consistent with physisorption, while those greater than  $-40 kJmol^{-1}$  correspond to chemisorption [42]. The calculated standard free energy of adsorption values for the Schiff

bases are in the range of  $-32$  and  $-34\text{kJ mole}^{-1}$  and it can be concluded that the adsorption of Schiff bases on the aluminium alloy surface is both physical and chemical, and chemisorption predominates [39, 43]. The sign of enthalpy and entropy of adsorption are positive and is related to substitutional adsorption, can be attributed to the increase in the solvent entropy and to a more positive water desorption enthalpy. The increase in entropy is the driving force for the adsorption of the Schiff bases on the aluminium alloy surface.

**Mechanism of inhibition:** The adsorption of organic molecules on the alloy surface cannot be considered only as purely physical or chemical adsorption phenomenon. In addition to the chemical adsorption, inhibitor molecules can also be adsorbed on the alloy surface via electrostatic interaction between the charged alloy surface and charged inhibitor molecule if it is possible [44]. The corrosion inhibition property of Schiff base through adsorption on the surface of the aluminium alloy can be attributed to the presence of electronegative atoms nitrogen and oxygen and also the presence of  $\pi$  electrons on the benzene ring. The alloy surface in contact with a solution is charged due to the electric field that emerges at the interface upon immersion in the electrolyte. This can be determined, according to Antropov et al [45] by comparing the zero charge potential and the rest potential of the alloy in the corresponding medium. The value of pHZch, which is defined as the pH at a point of zero charge is equal to 9.1 for aluminium [46], so aluminium is positively charged in highly acidic medium. The mechanism of adsorption of Schiff base can be predicted on the basis of the mechanism proposed for the corrosion of aluminium in hydrochloric acid [47]. According to this mechanism, anodic dissolution of aluminium involves following steps.



The cathodic hydrogen evolution involves the following steps.



In highly acidic solutions, the Schiff base molecule undergoes protonation and can exist as a protonated positive species. The protonated species gets adsorbed on the cathodic sites of the alloy surface through electrostatic interaction, thereby decreasing the rate of the cathodic reaction. The presence of anions in the solution and their adsorption on the alloy surface play an important role in the mechanism of inhibition exhibited by the organic compounds [48]. In a highly acidic medium like the one in the present investigation, the alloy surface is positively charged. The protonated species causes the negatively charged chloride ions to get adsorbed on the alloy surface, making the alloy surface negatively charged. The positively charged protonated Schiff base molecules interact electrostatically with the negatively charged chloride adsorbed alloy surface, resulting in physisorption. The negative charge centers of the Schiff base molecules containing a lone pair of electrons and  $\pi$ -electrons can electrostatically interact with the anodic sites on the alloy surface and get adsorbed. The neutral inhibitor molecules occupy the vacant adsorption sites on the alloy surface through the chemisorption mode involving the displacement of water molecules from the alloy surface and sharing of electrons by the hetero atoms like nitrogen and oxygen. The presence of Schiff base in the protonated form and the presence of negative charge centers on the molecule are also responsible for the mutual interaction of inhibitor molecules on the alloy surface.

In acidic solution, the nitrogen and oxygen atoms of the Schiff base molecules can adsorb on the cathodic sites of aluminium in competition with the hydrogen ions. The adsorption of Schiff base on the aluminium alloy surface can be attributed to adsorption of the organic compounds via phenolic and iminic groups in both cases. The adsorption will take place through the delocalized  $\pi$ -electrons of the phenolic group, iminic nitrogen and also through electron releasing group  $-\text{OCH}_3$ . Among these two Schiff bases, the chelate effect of Msalen is greater than that of Salen. This is attributed to the presence of two electron

releasing groups of  $-OCH_3$  in Msalen structure than Salen. The more efficient adsorption of Msalen is the result of electronegative oxygen atoms present in Msalen compared to Salen structure.

**Half-life ( $t_{1/2}$ ) values:** The half-life values give the information regarding the durability of inhibitor film on the surface of aluminium alloy under the studied corrosive conditions [49]. In the present study of corrosion of aluminium alloy in 1M hydrochloric acid, the weight of test specimen after a specific immersion time is designated as final weight ( $W_f$ ). A straight line was obtained for the plot of  $\log W_f$  versus immersion time in hours at 303K in absence and presence of Schiff base as shown in the Fig. 8 (a) and (b) the linear plots confirms signifying first-order kinetics [50,51]. The values of rate constant ( $k$ ) were calculated [52] from the following first order rate equation (17).

$$k = \frac{2.303}{t} \log \frac{W_i}{W_f} \quad \dots\dots\dots(17)$$

Where  $W_i$  is the initial mass of the test specimen and  $W_f$  is the final mass of the test specimen corresponding to time  $t$ .

The half-life value was calculated [53] using the equation (18).

$$t_{1/2} = \frac{0.693}{k} \quad \dots\dots\dots(18)$$

The values of rate constant ( $k$ ) and half-life ( $t_{1/2}$ ) period values are summarized in Table 7.

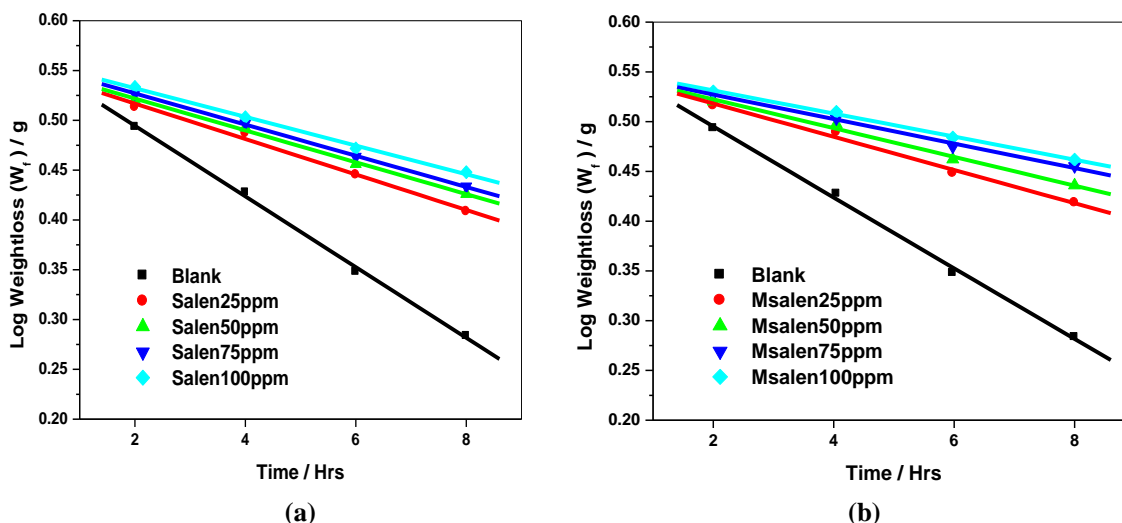


**Figure 8.** Plot of  $\log (W_f)$  versus immersion time for AA6061 alloy in 1M hydrochloric acid in absence and presence of (a) Salen and (b) Msalen at 303K.

**Table 7.** Half-Life values for AA6061 alloy in 1M hydrochloric acid in absence and presence of (a) Salen and (b) Msalen at different temperatures.

Inhibitor	Concentration (ppm)	Temperature							
		303K		313K		323K		333K	
		$k \times 10^{-3}$ ( $h^{-1}$ )	$t_{1/2}$ (h)	$k \times 10^{-3}$ ( $h^{-1}$ )	$t_{1/2}$ (h)	$k \times 10^{-3}$ ( $h^{-1}$ )	$t_{1/2}$ (h)	$k \times 10^{-3}$ ( $h^{-1}$ )	$t_{1/2}$ (h)
Salen	Blank	51.83	13.4	91.41	7.6	158.87	4.4	263.79	2.6
	25	19.07	36.3	40.89	16.9	82.70	8.4	152.17	4.6
	50	17.54	39.5	38.18	18.2	76.31	9.1	141.17	4.9
	75	15.50	44.7	35.48	19.5	70.01	9.9	127.76	5.4
	100	13.98	49.6	31.02	22.3	62.25	11.1	122.49	5.7
Msalen	25	17.54	39.5	37.28	18.6	76.31	9.1	146.64	4.7
	50	16.01	43.3	31.91	21.7	68.45	10.1	135.76	5.1
	75	14.49	47.8	29.24	23.7	63.79	10.9	125.12	5.5
	100	12.97	53.4	25.71	27.0	57.64	12.0	117.28	5.9

The results obtained revealed that the rate constant values decreased with increase in Schiff base concentration at a particular temperature and increased as the temperature increases. The half-life values increased with increase in concentration of the Schiff base, indicating decrease in the dissolution rate of the aluminium alloy with increase in concentration of Schiff base at particular temperature and decreased as the temperature increases indicating desorption of the inhibitor molecules from alloy surface at higher temperatures.

**Scanning electron microscopy (SEM):** The effect of corrosion on the surface morphology of the AA6061 alloy sample was analyzed by recording the SEM images of the alloy samples in 1M hydrochloric acid for 2 hours of immersion in the absence and presence of 100 ppm Salen and Msalen. Fig. 9 shows SEM images of (a) polished alloy with the characteristic features of the polishing lines, Fig. 9(b) damaged alloy with rough surface due to attack of hydrochloric acid and Fig.9 (c) and (d) AA6061 alloy in presence of 1M hydrochloric acid and 100 ppm Salen and Msalen. It can be seen that the alloy surface is less damaged in presence of Msalen than Salen compared to aluminium alloy surface dipped in 1M hydrochloric acid solution without inhibitor. Thus it can be concluded that Msalen protects the alloy effectively than Salen by forming a uniform film on the surface of alloy.

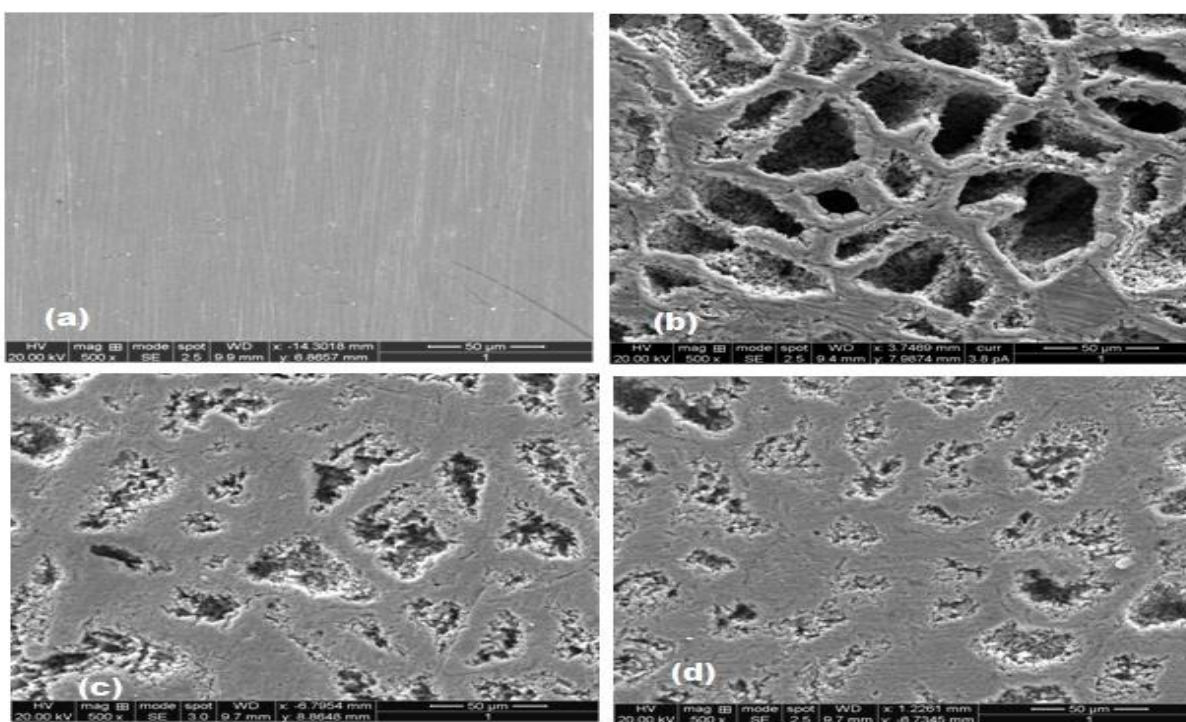


**Figure 9.** SEM images of (a) polished AA6061 alloy, (b) AA6061 alloy in 1M hydrochloric acid, (c) and (d) alloy in presence of (1M HCl +100ppm) Salen and Msalen.

**Atomic force microscopy (AFM):** The AFM is a powerful technique to investigate the surface topography at nano to micro-scale and has become a new choice to study the influence of inhibitor on the generation and the progress of the corrosion at the alloy/solution interface. Analysis of the images allowed quantification of surface roughness over area scales  $12 \times 12 \mu\text{m}^2$  and contained  $256 \times 256$  data points. Atomic force microscope was used mainly for measuring three-dimensional topography of the alloy surface. The three-dimensional AFM images of the alloy samples in 1M hydrochloric acid for 2 hours immersion in the absence and presence of 100 ppm Salen and Msalen are shown in Fig.10. The surface of polished aluminium alloy sample contain only the characteristic features of the polishing lines as shown in Fig.10(a), Fig.10(b) shows damaged alloy with rough surface due to attack of hydrochloric acid, Fig.10(c) and (d) shows less damaged alloy surface in presence of 1M hydrochloric acid and 100 ppm of Salen and

Msalen. The surface of aluminium alloy is less damaged in presence of Msalen than Salen compared to aluminium alloy surface dipped in 1M hydrochloric acid solution. The average roughness (Ra) values of polished aluminium alloy surface and, aluminium alloy in 1M hydrochloric acid without inhibitor was calculated to be 89 and 423 nm respectively. However, in presence of 100 ppm concentration of the Salen and Msalen, the average roughness was reduced to 329 and 311nm respectively.

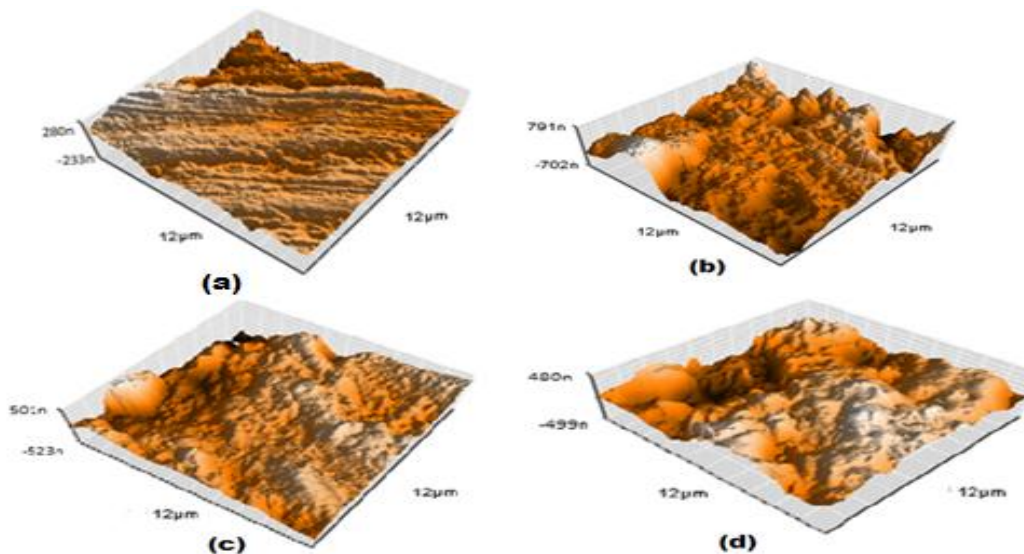


**Figure 10.** AFM micrographs of (a) polished AA6061 alloy, (b) AA6061 alloy in 1M hydrochloric acid, (c) and (d) in presence of (1M HCl +100ppm) Salen and Msalen

## APPLICATIONS

The study is useful to investigate the inhibition effect of some Schiff base compounds on the corrosion of AA60061 alloy in 1M HCl using weight loss, potentiodynamic polarization and electrochemical impedance spectroscopy techniques.

## CONCLUSIONS

- The inhibition efficiency of the Schiff bases increases with increase in inhibitor concentration, whereas decreases with increase in immersion time and temperature.
- The inhibition efficiency obtained using weight loss, potentiodynamic polarization, and EIS studies are in good agreement and in accordance to the order Msalen > Salen for AA6061.
- Potentiodynamic polarization studies demonstrate the Schiff bases under investigation act as mixed type but predominantly cathodic inhibitors.
- Impedance studies indicated that with increasing inhibitor concentration  $R_{ct}$  values increased, while  $C_{dl}$  values decreased. This shows that the inhibition may be due to surface adsorption of the inhibitor.
- The CPE exponent ( $n$ ) value increased with increase in inhibitor concentration is indicative of decrease in surface roughness of alloy surface.
- The values of enthalpy of activation ( $\Delta H^*$ ) are positive; this indicates that the corrosion process is endothermic and dissolution process of aluminum alloy decreases.



- The values of entropy of activation ( $\Delta S^*$ ) are higher in the presence of inhibitor than those in the absence of inhibitor. The increase in values of  $\Delta S^*$  reveals that an increase in randomness occurred on going from reactants to the activated complex.
- The  $E_a$  values of aluminium alloys in 1M Hydrochloric acid in the presence of all Schiff base compounds are higher than those in the absence of Schiff bases. The activation energies of the corrosion process are above  $20 \text{ kJmol}^{-1}$ , which is attributed to physical adsorption of inhibitor molecules.
- The negative values of  $\Delta G^\circ_{\text{ads}}$  indicate that the adsorption of the Schiff base molecule is a spontaneous process and the calculated standard free energy of adsorption values for the Schiff bases are closer to  $-40 \text{ kJ mole}^{-1}$  and it can be concluded that the adsorption of Schiff bases on the aluminium alloy surface is both physical and chemical, and chemisorption predominates. The adsorptions of Schiff bases on alloy surface in 1M HCl solution obeyed Langmuir adsorption isotherm.
- The inhibition is due to the adsorption of the Schiff base on the Alloy surface and blocking of active sites and adsorption of the Schiff base on the surface obeyed the Langmuir's adsorption isotherm.
- Schiff bases with methoxy groups showed higher inhibition efficiency for AA6061 alloy. This is attributed to the presence of two electron releasing groups of  $-\text{OCH}_3$ .
- Scanning Electron Microscopy (SEM) and Atomic Force Microscopy (AFM) images shows a smoother surface for inhibited alloy samples than uninhibited samples due to formation of protective barrier film.

### ACKNOWLEDGEMENTS

Authors would like to thank for their encouragement to Dr. M.A. Quraishi, Professor of Chemistry, IIT-(BHU), Varanasi, India, Dr. D.B. Fakruddin, Professor Emeritus, Siddaganga Institute of Technology, Tumkur, India, Thanks are due to Dr. Syed Abu Sayeed Mohammed, Prof. MN Zulfiqar Ahmed and Mr. Syed Nayazulla of department of Engineering Chemistry, Mrs. Soni. M. EEE department, HKBK College of Engineering, for their contribution during the experimental work.

### REFERENCES

- [1] Mountarlier, V., Gigandet, M.P., Normand, B., and Pagetti, J., *Corrosion Sci.*, **2005**, 47, 937.
- [2] Osman, M.M., Khamis, E., and Michael. A., *Corros. Prev. Control*, **1994**, 41, 60.
- [3] Bilgic, S. and Caliskan, N, *J. Appl. Electrochem*, **2001**, 31, 79.
- [4] Quraishi, M. A and Sardar, R., *Corrosion Sci*, **2002**, 58, 103.
- [5] Quraishi, M.A. and Jamal, D. Dianils, *Mater. Chem. Phys.*, **2003**, 78, 608.
- [6] M.N. Dasai, C.B. Shah, Y.B. Desai, S.M. Desai and M.H.Gandhi, *Br. Corros. J.*, **1963**, 4, 15.
- [7] Kumar Mahor Devender, Kumar Upadhyay Rajesh and Chaturvedi Alok, *Rev. Roum. Chim*, **2010**, 55(4), 227.
- [8] Nabel A. Negm, Mohamed F. Zaki, *Colloids and Surfaces A: Physicochemical and Engineering Aspects*, **2008**, 322, 1-3, 97-102.
- [9] H. Ashassi-Sorkhabi, B. Shabani, B. Aligholipour, D. Seifzadeh, *Applied Surface Science*, **2006**, 252(12), 4039-4047.
- [10] M.N. Desai, M.M. Pandya and G.V. Shah, *Indian. J. Technol.*, **1981**, 19, 292
- [11] Aluminum Association Publication T-8, The Aluminum Association, Washington, DC, **1979**.
- [12] S. Zolezzi, A Decinti, E. Spodine, *Polyhedron*, **1999**, 18(6), 897-904.
- [13] T. Z. Yu, W. M. Su, W. L. Li, Z. R. Hong, R. N. Hua, M. T. Li, B. Chu and B. Li, *Inorg. Chem. Acta*, **2006**, 359, 2246.
- [14] Standard Practice for Laboratory Immersion Corrosion testing of Metal-G31-72-**2004**.
- [15] Ferreira E.S., Giacomelli C., Giacomelli F.C. and Spinelli A., *Mater. Chem. Phys.*, 83, 129-134.

- [16] W. H. Li, Q. He, S. T. Zhang, C. L. Pei, and B. R. Hou, *Journal of Applied Electrochemistry*, **2008**, 38(3), 289–295.
- [17] A. Yurt, S. Ulutas, H. Dal, *Applied Surface Science*, **2006**, 253(2), 919-925.
- [18] M. Metikos-Hukovic, R. Babic, Z. Grubac, *J. Appl. Electrochem*, **1998**, 28, 433-440.
- [19] A. Aytac, U. Ozmen, M. Kabasakaloglu, *Materials Chemistry and Physics*, **2005**, 89-1, 176-181.
- [20] Brett C. M. A., *J. Appl. Electrochem.*, **1990**, 20, 1000-1006.
- [21] Brett C. M. A., *Corros. Sci.*, Vol **33**(2), 1992, pp 203-208.
- [22] M. Metikos-Hukovic, R. Babic, Z. Grubac, *J. Appl. Electrochem*, **1998**, 28, 433-440.
- [23] E.J. Lee, S.I. Pyun, *Corros. Sci.* **1995**, 37, 157–168.
- [24] K.F. Khaled, M.M. Al-Qahtani, *Mater. Chem. Phys.*, **2009**, 113, 150-158.
- [25] A. Ehteram Noor, *Mater. Chem. Phys*, Vol 114, 2009, pp 533-540.
- [26] T. Pajkossy, *J. Electronal. Che.* **1994**, 364, 111-118.
- [27] W.R. Fawcett, Z. Kovacova, A. Mtheo, C. Foss, *J. Electronal. Chem*, **1992**, 326, 1-2.
- [28] R. de Levie, *Electrochem. Acta.*, Vol 8,1963, pp 751-780.
- [29] H.J.W. Lenderink, M.V.D. Linden, J.H.W. De Wit, *Electrochim. Acta*, **1989**, 38, 1993-2000.
- [30] F. Mansfeld, C.H. Tsai, H. Shih, in: R.S. Munn (Ed.), *Computer Modeling in Corrosion*, ASTM, Philadelphia, PA, **1992**, 86-95.
- [31] C.H. Hsu, F. Mansfeld, *Corrosion*, 57 Edition, **2001**, 747-755.
- [32] M.A Quraishi. Rawat, *J Corrosion*. **2001**, 19, 273-280.
- [33] Fouda, AS, Heakal, FE, Radwan, MS, *J. Appl. Electrochem.*, **2009**, 39, 391–402.
- [34] H. Ashassi-Sorkhabi, B. Shaabani, D. Seifzadeh, *Appl. Surf. Sci.* **2005**, 239, 154-160.
- [35] F. Mansfeld, *Corrosion Mechanism*, Marcel Dekkar, New York, **1987**, 119-125.
- [36] Poornima, T, Nayak, J, Shetty AN, *J. Appl. Electrochem.*, **2011**, 41, 223–233.
- [37] Ashish Kumar Singh, M.A. Quraishi, *Corros. Sci.* **2010**, 52, 1529-1535.
- [38] E.A.Noor, A.H. Al-Moubaraki., *Mater.Chem. Phys*, **2008**, 110, 145.
- [39] A. Yurt, A. Balaban, S.U. Kandemir, G. Bereket, B. Erk, *Mater. Chem. Phys*, **2004**, 85, 420-425.
- [40] G.E. Badr, *Corros. Sci.*, **2009**, 51, 2529-2536.
- [41] T. Pajkossy, *J. Electronal. Chem*, **1994**, 364, 111-120.
- [42] Fuchs, GR, *Colloids Surf.*, **2006**, 280, 130-138.
- [43] Hosseini, M, Mertens, SFL, Arshadi, MR, *Corros. Sci.*, **2003**, 45, 1473–1482.
- [44] Ashish Kumar Singh, M. A. Quraishi., *Int. J. Electrochem. Sci.*, **2012**, 7, 3222-3241.
- [45] Antropov, L.I., Makushin, E.M. and Panasenko, V.F, *Kiev, Technika*, **1981**, 34, 182-189.
- [46] Tschapek, M.C., Wasowski, R.M. and Torres Sanchez., *J. Electroanal. Chem.*, **1976**. 74, 167-176.
- [47] Awady, A.A., Abd. El- Nabey, B.A. and Aziz, S.G. *J. Chem. Soc. Faraday Trans.*, **1993**, 89, 795-802.
- [48] Hackerman, N, Snavely, ES, Jr, Payne, JS, Jr., *Electrochem. Soc.*, **1966**, 113, 677–686.
- [49] Orubite, Okorasaye K., and Oforka N. C., *J. Appl. Sci. Environ.*, **2004**, 8-1, 57-61.
- [50] Ekpe.U.J, Ebenso. E.E, Ibok. UJ. W.Afri.SciAssoc, **2004**, 37, **1994**, 13-30.
- [51] Ibok. U., Ekpe.U.J, and Ita, O.E, *Mat. Chem. And Phy*, **2004**, 40, **1994**, 63-70.
- [52] Adnan S. Abdul Nabi, Luma T. Tomaa, Ishan A. Mikshif., *J. Thi-Qar Sci.*, **2010**, 2(1), 71-76.
- [53] P.W. Atkins, “Chemisorbed and Physisorbed Species- A Textbook of Physical Chemistry”, University Press, Oxford **1980**, 936.